Two-dimensional array of diffractive microlenses fabricated by thin film deposition

Jürgen Jahns and Susan J. Walker

A 2-D array of 10 × 10 diffractive lenslets was fabricated and tested. Each lenslet has a rectangular aperture and a size of 1.5 mm × 1.5 mm. The focal length of each lenslet is 47 mm. The array was produced by depositing thin films of silicon monoxide on a quartz glass substrate and by using photolithographic techniques. The performance of the lenslets is based on the diffraction of light at a Fresnel zone plate (FZP). The FZP pattern was implemented as a phase structure with eight discrete levels. The diffraction efficiency was measured to be 91%. *Key words*: microlenses; microlithography; thin films; diffraction.

I. Introduction

Microlenses are becoming standard optical components with current applications in laser printers, facsimile machines, and in optical communications. Future use might lie in the field of optical interconnections in VLSI systems or in optical computing systems. A variety of possibilities exists for the fabrication of microlenses. We can distinguish between refractive[1–7] and diffractive lenses[8–12] depending on the implementation of the lens performance. We are interested in the use of microlenses in optical computing systems, for applications such as array illumination[13] and optical interconnections.[14] Specifically, we are interested in diffractive lenses since they are computer generated structures which offer great flexibility for their design. Diffractive lenses can be manufactured in a wide variety of sizes and geometrical shapes. For example, it is possible to give the lenslets in an array a rectangular shape and, therefore, obtain a fill factor of the available area of 100%.

The action of a diffractive lens is based on near field diffraction at a Fresnel zone plate (FZP). A high diffraction efficiency can be achieved by implementing the FZP pattern as a blazed phase structure, as it was proposed by Dammann in 1970.[8] For the fabrication of arrays of diffractive lenses, photolithographic techniques are convenient since they allow all lenslets to be made in parallel with a resolution that is sufficient for many applications. The fabrication of diffractive lenses using the deposition of thin dielectric films was first demonstrated by d'Auria *et al.*[9]

In this paper, we will describe the properties of a 2-D array of diffractive lenslets fabricated with eight discrete phase levels. The lenslets were realized by deposition of thin layers of silicon monoxide (SiO) using optical lithography. We shall begin by describing the theory of diffractive lenses (Sec. II), then the fabrication process using thin film deposition (Sec. III), and finally show some experimental results (Sec. IV).

II. Theory of Diffractive Lenses

As we mentioned earlier, the action of a diffractive lens is based upon near field diffraction by an FZP. A Fresnel zone plate is a binary amplitude pattern which is formed by a series of concentric rings [Fig. 1(a)]. The radius of the mth transparent ring is determined by the square root of its index m:

$$r_m = \sqrt{m} r_p \tag{1}$$

Obviously, an FZP is periodic in r^2 with a period r_p^2. Figure 1(b) shows the profile of an FZP as a function of r^2.

When an FZP is illuminated by a plane monochromatic wave of wavelength λ, a multitude of diverging and converging spherical waves can be observed behind the FZP (Fig. 2). Each wave represents one diffraction order whose amplitude and focal length are determined by the FZP pattern. The undiffracted light which passes through the FZP forms the zeroth order. We now want to derive equations for the z-coordinates of the focal planes and for the amplitudes of the diffraction orders using scalar diffraction theory. We do this for the general case of a component which is periodic in r^2 without any further assumptions about its amplitude or phase distribution.

The authors are with AT&T Bell Laboratories, Crawfords Corner Road, Holmdel, New Jersey 07733.

Received 24 April 1989.
0003-6935/90/070931-06$02.00/0.

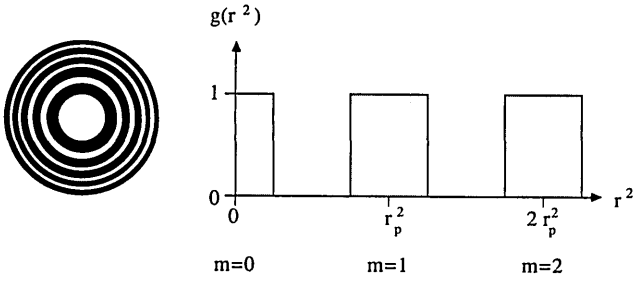

Fig. 1. Fresnel zone pattern (a) and its amplitude transmission as a function of r^2 (b).

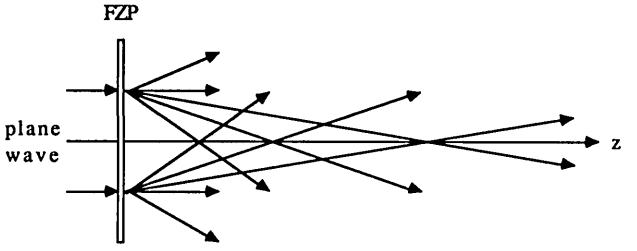

Fig. 2. Diffraction of a plane wave at a Fresnel zone plate.

We denote the complex amplitude transmittance of the FZP component by $g(x,y)$. Since it has radial symmetry and is periodic in r^2, we may write:

$$g(x,y) = g(x^2 + y^2) = g(r^2) = g(r^2 + jr_p^2). \tag{2}$$

In this equation j denotes an arbitrary integer. It should be noted that by writing Eq. (2), we formally extend the range of r^2 to negative values. This formal trick is convenient for the mathematical treatment of our problem. Since the extension to negative values of r^2 does not change the physical situation, it also does not affect our results. Based on the r^2 periodicity, we can represent $g(x,y)$ mathematically as a Fourier series:

$$g(x,y) = \sum_{n=-\infty}^{\infty} A_n \exp\left(2\pi i n \frac{x^2 + y^2}{r_p^2}\right). \tag{3}$$

The Fourier coefficients A_n are computed to be:

$$A_n = (1/r_p^2) \int_0^{r_p^2} g(r^2) \exp(-2\pi i n r^2) d(r^2). \tag{4}$$

As we shall see, these Fourier coefficients give the values of the amplitudes of the foci of the FZP. We assume that $g(x,y)$ is positioned in a plane $z = 0$ and illuminated by a plane wave. Then the complex amplitude $u(x',y',z)$ of the diffracted light in any plane with $z > 0$ is given by the Fresnel integral:

$$u(x',y',z) = \int\int g(x,y) \exp\left\{\frac{i\pi}{\lambda z}[(x - x')^2 + (y - y')^2]\right\} dxdy. \tag{5}$$

Here, some unimportant factors were dropped. The integration boundaries go from $-\infty$ to ∞ if we assume infinite extension for $g(x,y)$. By inserting Eq. (3), we obtain:

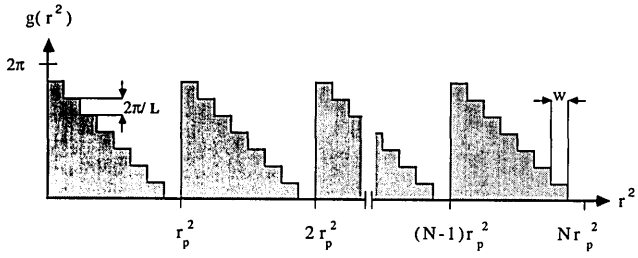

Fig. 3. Phase profile of a diffractive lens with multiple discrete phase levels.

$$u(x',y',z) = \sum_{(n)} A_n \exp\left[\frac{i\pi}{\lambda z}(x'^2 + y'^2)\right] \times \int\int \exp\left[2\pi i\left(\frac{n}{r_p^2} + \frac{1}{2\lambda z}\right)(x^2 + y^2)\right] \times \exp\left[2\pi i\left(\frac{xx' + yy'}{\lambda z}\right)\right] dxdy. \tag{6}$$

The integral in Eq. (6) yields a delta peak on the optical axis (i.e., for $x' = y' = 0$), if $n/r_p^2 + 1/(2\lambda z) = 0$. These peaks are the foci generated by the FZP. For $z = z_n$ with

$$z_n = -\frac{r_p^2}{2\lambda n}, \tag{7}$$

we can therefore write:

$$u(x',y',z_n) = A_n \exp\left[\frac{i\pi}{\lambda z_n}(x'^2 + y'^2)\right] \delta\left(\frac{x'}{\lambda z_n}, \frac{y'}{\lambda z_n}\right) + \sum_{m \neq n} A_m \cdot \tag{8}$$

Planes $z = z_n$ with $n = 0, \pm 1, \pm 2, \ldots$ are the focal planes of the FZP. The amplitude of the wave focussed to plane z_n is A_n. The sum in Eq. (8) with $m \neq n$ represents the waves that are diffracted into other planes, $z = z_m$. So far, we have assumed infinite extension of the FZP. If the FZP is rectangular with widths w_x and w_y, respectively, in x- and y-direction, the delta-function in Eq. (8) becomes replaced by a sinc-function:

$$u(x',y',z_n) = A_n \exp\left[\frac{i\pi}{\lambda z_n}(x'^2 + y'^2)\right] \operatorname{sinc}\left(\frac{x'w_x}{\lambda z_n}, \frac{y'w_y}{\lambda z_n}\right). \tag{9}$$

In the case shown in Fig. 3, it is $w_x = w_y = \sqrt{N} r_p$. Note, that, according to Eq. (7), z_n becomes negative for $n > 0$. This corresponds to a spherical wave diverging from the FZP. Negative values of n yield the z-coordinates of the focal planes of the FZP. For $n = 0$, z_n becomes infinite. This corresponds to a plane wave which represents the zeroth diffraction order.

As we mentioned earlier, Eq. (8) holds for all components which are periodic in r^2. We are interested especially in multilevel phase components with discrete phase levels. A positive lens with a quantized phase profile (Fig. 3) can be represented mathematically as:

$$g(r^2) = \sum_{k=0}^{N(L-1)} \exp\left(\frac{-2\pi i k}{L}\right) \operatorname{rect}\left(\frac{r^2 - kr_p^2/L - r_p^2/2L}{r_p^2/L}\right). \tag{10}$$

Here, L denotes the number of phase levels. For simplicity, a constant phase factor $\exp[2\pi i(L - 1)/L]$

was omitted in Eq. (10). It is assumed, that the phase steps are all of equal height which is $2\pi/L$. In the following, we furthermore normalize the period, i.e. $r_p^2 = 1$. Then, using Eq. (4), we obtain for the amplitude of the nth diffraction order:

$$A_n = \int_0^1 \sum_{k=0}^{L-1} \exp\left(\frac{-2\pi i k}{L}\right) \operatorname{rect}\left(\frac{r^2 - k/L - 1/2L}{1/L}\right) \exp(-2\pi i n r^2) d(r^2). \tag{11}$$

$$= \exp\left(\frac{i\pi n}{L}\right) \operatorname{sinc}(n/L) \frac{1}{L} \sum_{k=0}^{L-1} \exp\left[2\pi i \frac{k(n+1)}{L}\right]. \tag{12}$$

The sum on the right side of Eq. (12) is zero unless $n + 1$ is a multiple of L.

$$\sum_{k=0}^{L-1} \exp\left[2\pi i \frac{k(n+1)}{L}\right] = \begin{cases} L & \text{if } n = jL - 1, j \text{ integer} \\ 0 & \text{else} \end{cases} \tag{13}$$

We are especially interested in the case $n = -1$ which corresponds to the first focal plane. The intensity of the wave diffracted into this plane is given as $|A_{-1}|^2$. This value is equal to the diffraction efficiency which we denote by η.

$$\eta = |A_{-1}|^2 = \operatorname{sinc}^2(1/L) = \left\{\frac{\sin(\pi/L)}{\pi/L}\right\}^2. \tag{14}$$

Figure 4 represents the values of $\eta(L)$ graphically. It is interesting, that the efficiency grows rapidly with L and is as high as 95% for an eight-level lens. At the same time, by increasing L the light intensity which is diffracted into other orders is reduced. This is visualized by Fig. 5 which shows the spectrum of the foci of a diffractive lens as a function of the phase level L.

We would like to add a remark which is important for the understanding of diffractive lenses. A phase structure, as shown in Fig. 3 with a stepped phase profile, can be considered as an approximation to the quadratic phase profile of a refractive lens. However, we have to keep in mind that the action of an FZP lens is based on diffraction rather than refraction. This means that the shape of the emerging wavefronts is determined only by the lateral FZP pattern, i.e., by the transition coordinates between different rings. Given a perfect pattern generation and lithography, a component as shown in Fig. 3, therefore generates perfect spherical waves. There are no deformations due to the stepped phase profile. This is demonstrated by the profile of the focal spot which is generated by a diffractive lens (see Sec. IV). The situation is comparable to conventional phase gratings as they are used, for array illumination, for example. There, the generated diffraction orders are also perfect plane waves even though the grating may have only two different phase values.

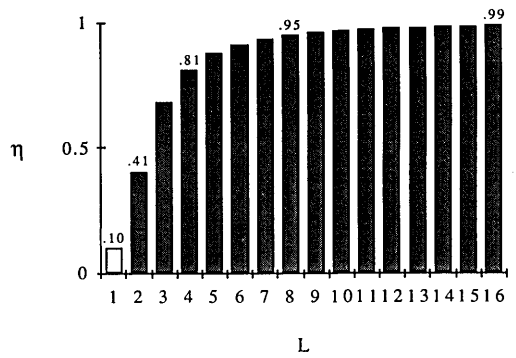

Fig. 4. Efficiency of a diffractive lens as a function of the number of phase levels. Note that for $L = 1$ the efficiency of a binary amplitude FZP is shown for comparison.

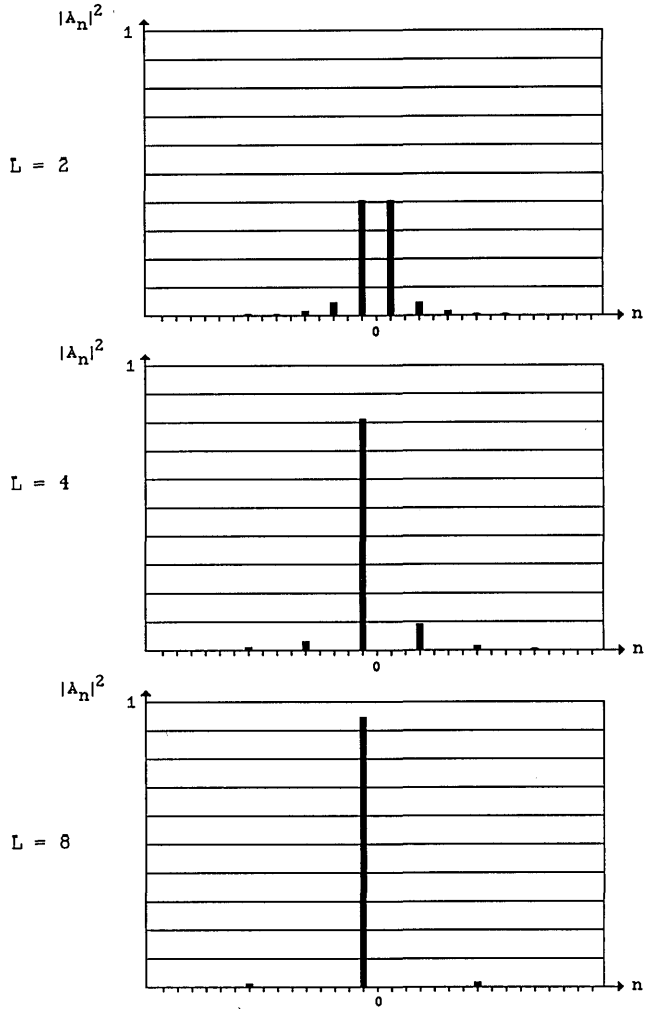

Fig. 5. Focal spectrum of a diffractive lens as a function of the number L of phase levels.

III. Fabrication of Multilevel Phase Structures Using Thin Film Deposition

The various steps included in the fabrication of a diffractive lens using thin film deposition are described in Fig. 6. The substrate, which in our case was quartz glass, is first coated with a film of photoresist (AZ 4210). Using standard optical lithography, a pattern is transferred into the resist. Then a layer of SiO was deposited in an evaporation chamber. The thickness of the layer has to be controlled, either by appropriate timing or by *in situ* monitoring of the deposition process, to achieve the desired phase shift. Silicon

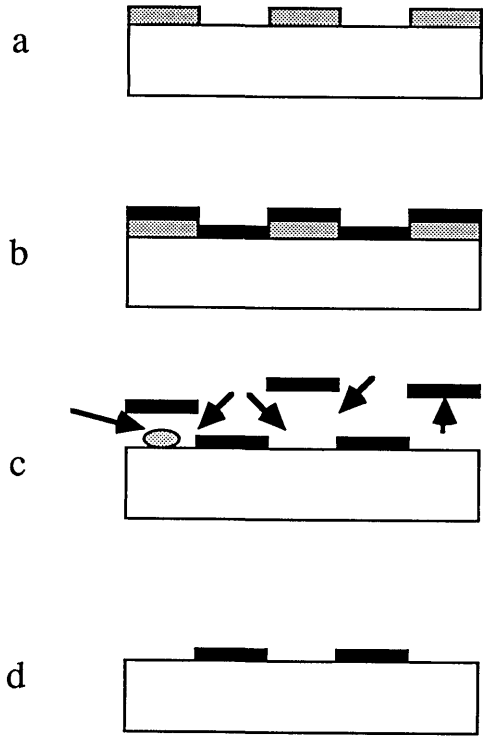

Fig. 6. Fabrication steps to generate a phase grating using thin film deposition: (a) resist patterning; (b) thin film deposition; (c) lift-off; and (d) resulting phase structure.

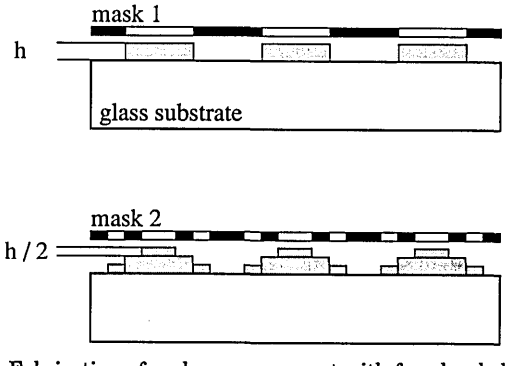

Fig. 7. Fabrication of a phase component with four levels by two successive steps.

monoxide was chosen as the deposited material because it is relatively easy to handle and because it gives a robust structure. A problem which might be associated with the use of SiO is that during the evaporation process, higher oxides (SiO_x) may be formed. This would result in a varied refractive index of the layer. This, in turn, would make it harder to produce the appropriate phase shift if the thickness of the layer is controlled by the time of the evaporation process.

After the deposition step, the sample is put in an acetone soak to remove the resist. It is important to note that for this technique to work the resist layer has to be thicker than the layer of deposited material. In this case, the acetone dissolves the resist from the side, seeps under the deposited material, and carries it away. What remains is a structured layer of SiO with a

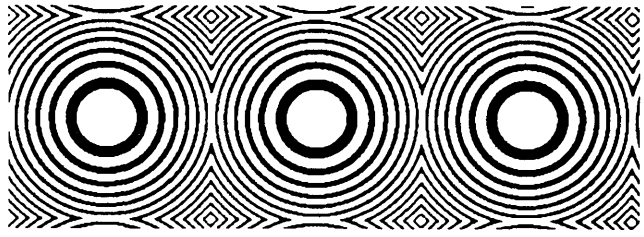

Fig. 8. Section of one of the mask patterns used for the fabrication of the lenslet array shown in Fig. 9.

certain thickness. By repeating the process several times, we can generate multilevel phase components. It is important to note, that to create a structure with 2^k discrete levels, only k repetitive steps are required. This is achieved by a binary decomposition of the final phase pattern as visualized in Figure 7. The thickness of the first layer h is chosen such that it yields a phase shift of π. The thickness of the remaining deposited layers then gets smaller from one step to the next by a factor of two.

To fabricate multilevel phase structures, a critical step for the fabrication is the proper alignment of the lithography mask with respect to the structure which was generated in the previous step. This can be done by placing appropriate alignment marks on the mask. In general, it is possible to achieve a positioning accuracy in the submicron range.

The pattern generation process to create the mask(s) which are involved in the process is done by computer. The mask itself is then made by an electron beam writer which results in a very good resolution (typically 0.1 μ). A part of the mask which was used to fabricate one layer of the lenslets is shown in Fig. 8.

The resolution which is required to fabricate a diffractive lens is determined by the f-number (*f/no.*) of the lens. This can be understood from Fig. 3 which shows the relevant parameters. If we assume a lens of circular aperture which consists of N periods in radial direction, the radius is given as $\sqrt{N}r_p$. For a structure with L phase levels, the minimum feature size w is approximately determined by the following equation:

$$w = \frac{r_p}{L}(\sqrt{N} - \sqrt{N-1}). \tag{15}$$

By developing $\sqrt{N-1}$ in a power series and dropping the higher terms, this expression becomes:

$$w = \frac{r_p}{2L\sqrt{N}}. \tag{16}$$

As for a refractive lens, we define the *f/no.* of a diffractive lens to be the ratio of focal length and the diameter:

$$f/no. = \frac{r_p^2/2\lambda}{2\sqrt{N}r_p} = \frac{r_p}{4\sqrt{N}\lambda}. \tag{17}$$

With Eq. (17), we can express the minimum feature size for a diffractive lens with L phase levels as:

$$w = \frac{2\lambda f/no.}{L}. \tag{18}$$

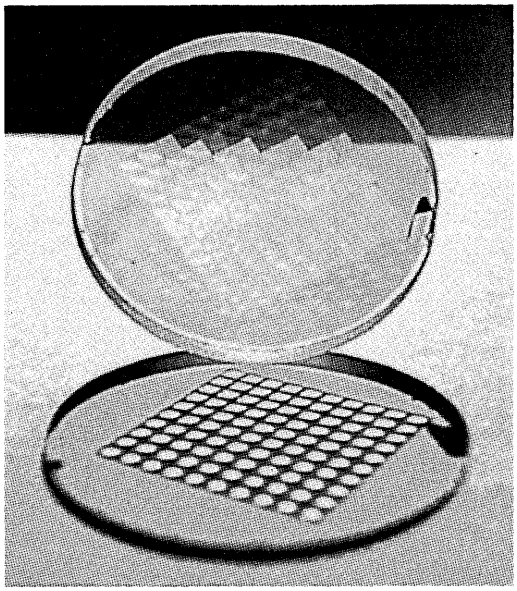

Fig. 9. Array of 10 × 10 lenslets on a one inch quartz glass substrate.

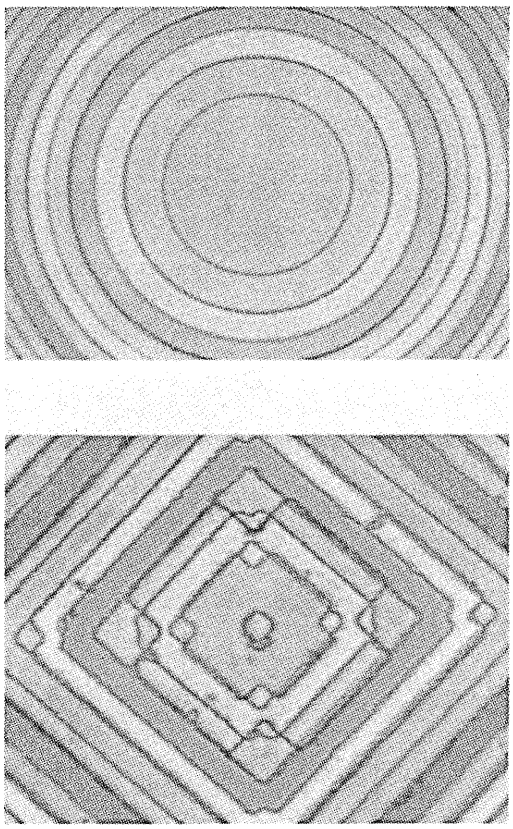

Fig. 10. Center of one lenslet (a) and corner between lenslets (b).

As an example, to make an f/8 lens with eight phase levels for a wavelength of 1 μm, we need a lithography with a resolution of 2 μm. This is achievable with current technology.

IV. Experimental Results

Figure 9 shows a picture of an array consisting of 10 × 10 rectangularly shaped lenslets. The substrate is made of quartz glass and has a diameter of 25.4 mm. The size of each individual lenslet is 1.5 mm × 1.5 mm. The focal length is 46.5 mm. This corresponds to a lens with f/31.

In Figure 10(a), we see a top view of the center of one lenslet and 10(b) shows a corner. In the picture we can recognize that several thin film layers were superimposed. The smallest features that were required for the fabrication of these lenslets are 5 μm.

In Figs. 11 and 12, the focal spots are shown as they are formed by the lenslets when illuminated by a plane

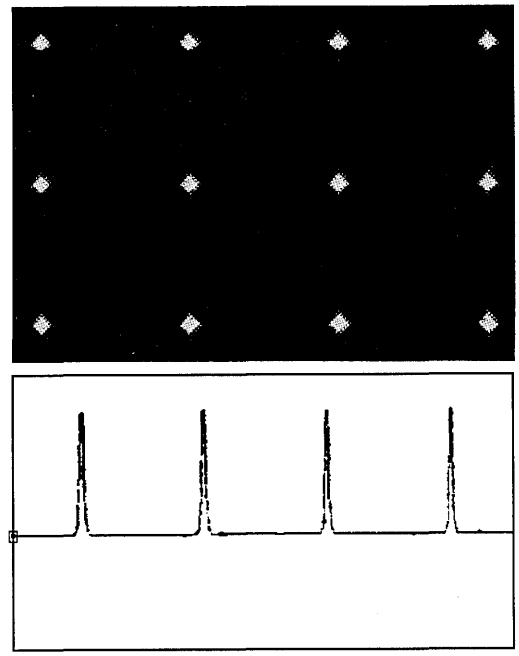

Fig. 11. Focal spots (a) and intensity profile (b).

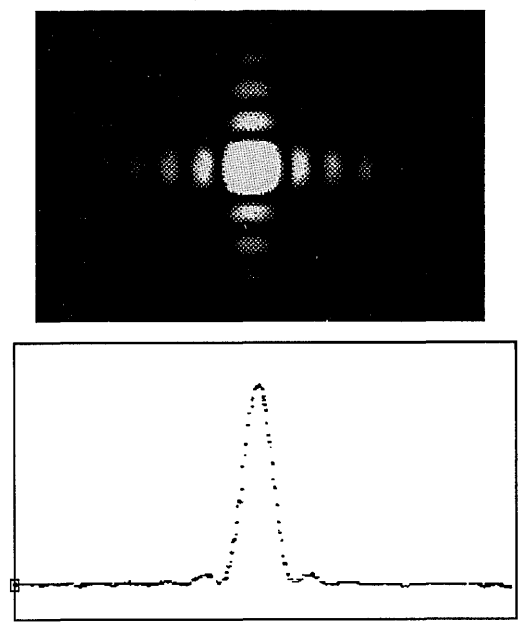

Fig. 12. Magnified view of one spot (a) and intensity profile (b).

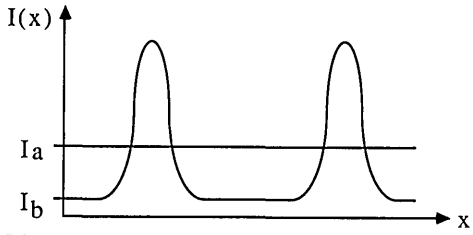

Fig. 13. Measurement of the diffraction efficiency was done by measuring the light intensity I_a without the lenslets being present and, in a second step, the intensity between the focal spots I_b.

monochromatic wave. Due to the rectangular shape of the lenslets, each focal spot has a $\mathrm{sinc}^2(\ldots)$-intensity profile. The central lobe has a width of 53 μm.

The diffraction efficiency was measured to be 91% which is close to the theoretical value for an eight-level lens. The measurement was made by illuminating the lenslets with a plane wave and measuring the intensity in the focal plane. Two measurements were taken: first, the constant intensity I_a was measured without the lenslet array being present (see Fig. 13). Then the lenslet array was inserted and the background intensity I_b between the focal spots was measured. To compensate for losses due to Fresnel reflection, I_a was measured with a blank glass substrate put in the optical setup. The diffraction efficiency was calculated as

$$\eta = \frac{I_a - I_b}{I_a} . \tag{19}$$

This definition is in agreement with the one given in Eq. (14). According to Eq. (19), η is 1 if I_b is zero, i.e., if all the light is collected in the focal spots. It is zero if $I_b = I_a$, i.e., if the lenslets have no focusing power at all.

V. Conclusion

We have described the fabrication of diffractive lenslets using a blazed multilevel phase structure. A 10 × 10 array of lenslets was demonstrated using thin films of SiO to make the phase structure. The measured diffraction efficiency which was obtained was 91%, which is close to the theoretical value for an eight-level lens. It exceeds the value which was reported by Shiono *et al.*[11] for a Fresnel lens fabricated by electron beam lithography (74%).

We presented a theory for diffractive lenslets to show the relationship between the various parameters of diffractive lenses as the focal length, diffraction efficiency, *f/no.*, and fabrication parameters, such as the number of phase levels and the spatial period of the FZP pattern.

The good performance of the lenses which were demonstrated here makes it interesting to use diffractive lenses for different purposes such as array illumination[13] and planar integration of free-space optical components using single substrates.[15] A feature of diffractive lenses which makes them interesting for a variety of applications is that, being computer generated structures, they offer a large flexibility in the design and fabrication of optical components and systems.

References

1. T. Uchida, M. Furukawa, I. Kitano, K. Koizumi, and H. Matsamura, "Optical Characteristics of a Light-Focusing Fiber Guide and its Applications," IEEE J. Quantum Electron. **QE-6**, 606–612 (1970).
2. L. G. Cohen and M. V. Schneider, "Microlenses for Coupling Junction Lasers to Optical Fibers," Appl. Opt. **13**, 89–94 (1974).
3. K. Iga, M. Oikawa, S. Misawa, J. Banno, and Y. Kokubun, "Stacked Planar Optics: An Application of the Planar Microlens," Appl. Opt. **21**, 3456–3460 (1982).
4. F. W. Ostermayer, P. A. Kohl, R. H. Burton, and C. L. Zipfel, "Photochemical Formation of Integral Lenses on InP/InGaAsP LEDs," in *Proceedings IEEE Conference on Light Emitting Diodes and Photodetectors* (1982).
5. O. Wada, "Ion-Beam Etching of InP and its Applications to the Fabrication of High Radiance InGaAsP/InP Light Emitting Diodes," J. Electrochem. Soc. **131**, 2373–2380 (1983).
6. N. F. Borrelli and D. L. Morse, "Microlens Arrays Produced by a Photolytic Technique," Appl. Opt. **27**, 476–479 (1988).
7. Z. D. Popovic, R. A. Sprague, and G. A. Neville Connell, "Technique for Monolithic Microlens Fabrication," Appl. Opt. **27**, 1281–1284 (1988).
8. H. Dammann, "Blazed Synthetic Phase-Only Holograms," Optik **31**, 95–104 (1970).
9. L. D'Auria, J. P. Huignard, A. M. Roy, and E. Spitz, "Photolithographic Fabrication of Thin Film Lenses," Opt. Commun. **5**, 232–235 (1972).
10. A. H. Firester, D. M. Hoffman, E. A. James, and M. E. Heller, "Fabrication of Planar Optical Phase Elements," Opt. Commun. **8**, 160–162 (1973).
11. T. Shiono, K. Setsune, O. Yamazaki, and K. Wasa, "Rectangular-Apertured Micro-Fresnel Lens Arrays Fabricated by Electron-Beam Lithography," Appl. Opt. **26**, 587–591 (1987).
12. J. R. Leger, M. L. Scott, P. Bundman, and M. P. Griswold, "Astigmatic Wavefront Correction of a Gain-Guided Laser Diode Array Using Anamorphic Diffractive Microlenses," Proc. Soc. Photo-Opt. Instrum. Eng. **884**, 82–89 (1988).
13. J. Jahns, N. Streibl, and S. J. Walker, "Multilevel Phase Structures for Array Generations," OE/LASE '89, Los Angeles, Jan. 15–20, 1989.
14. J. Jewell and S. L. McCall, "Microoptic Systems: Essential for Optical Computing," Topical Meeting on Optical Computing, Salt Lake City, Feb. 27–March 1, 1989.
15. J. Jahns and A. Huang, "Planar integration of free-space optical components," Appl. Opt. **28**, 1602–1605 (1989).